Turkish Online Journal of Qualitative Inquiry (TOJQI)
Volume 13, Issue 1, January 2022: 823-835

Comparative Analysis of Power Factor Corrected HBLLC and PSFB Converter for an Electric Vehicle Charger Application by using CUK Converter

K. Lakshman Pavan, J. Somlal
Student of M. Tech, final year, Department of Electrical and Electronics Engineering, K L University, Vaddeswaram, Guntur, Andhra Pradesh, India.
Professor, Department of Electrical and Electronics Engineering, K L University, Vaddeswaram, Guntur, Andhra Pradesh, India.
lakshmanpavankanduri@gmail.com, jarupulasomu@kluniversity.in

Abstract:
The need of clean and green environment, existing transport system changes into Electric vehicles. For those EV's we need fast and efficient charger. This work represents an improved power quality CUK converter fed Phase Shift Full Bridge converter and HBLLC converter for an on-board battery charger used in electric vehicle application. This topology consists of two converters, one for Power factor correction and another one for electric vehicle battery charging by using CC and CV algorithm. In this topology, the CUK converter is used for Power factor correction and Phase Shift Full Bridge converter and HBLLC converter is used for conversion of dc-link voltage to the dc voltage that is required for the battery charging. This Proposed Converter was designed and simulated in MATLAB/SIMULINK to transform 300 V input voltage to an output voltage range of 48-55V at 580W and comparing the values taking all parameters into account step by step.
Keywords: CUK Converter, Half Bridge LLC (HBLLC), Phase Shift Full Bridge converter (PSFB), Power Factor Correction (PFC).

I. INTRODUCTION

The need of green and clean environment the transportation sector shifted into the Battery driven electric vehicles (BEV). The conventional transport has depended on the petroleum, diesel there is day by day increase of prices of these fuels. These IC engines produce hazardous greenhouse gas emissions.

For those above concern's, the electric vehicles are the only solution to address all those issues. In those battery powered vehicles are more dominant in that electric vehicle technology. The battery driven vehicles have On-board/Off-board charger for charging the vehicle from external source like charging stations with different types of charging technologies available in existence. In recent vehicles they have battery energy storage systems while charging system incorporate with power electronic circuit interfacing to it.

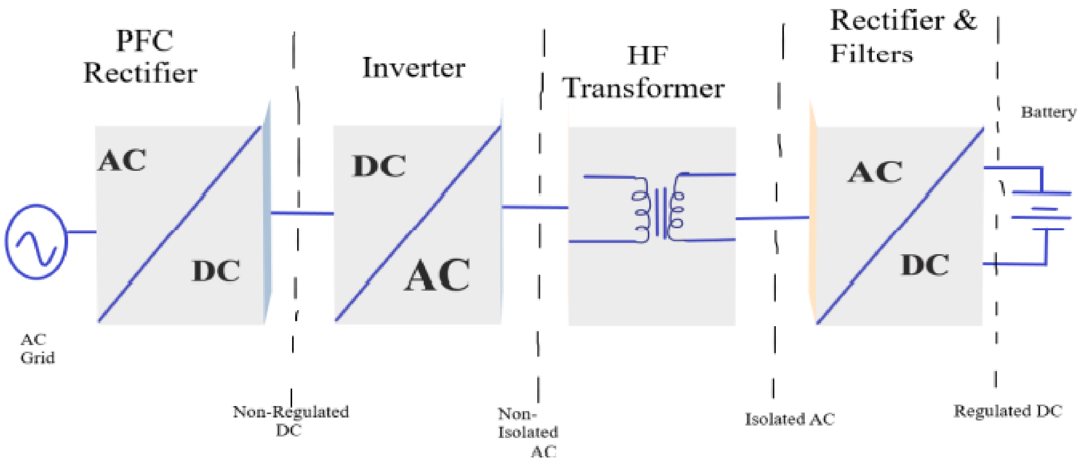

Fig. 1: EV Charging Circuit using PFC and HF Transformer

Fig.1 shows the modified EV charging Circuit. Here the AC supply is converts to DC by using the DBR and PFC in the first stage and it is connected to DC-link Capacitor to maintain constant DC output voltage. That DC voltage is fed to inverter it gives output as AC in these there is no isolation. For isolation purpose we are giving this AC supply to high frequency (HF) isolated transformer. It gives isolated AC as output and then giving DC to EV battery with rectifier and filters are connected to the secondary of transformer [1]. There are various topologies of converters among those phase-shifted zero voltage switching converter offers high efficiency due to the use of zero voltage switching scheme and it is suitable for wide input and output voltage variations for high power applications [2-4]. However, LLC resonant converters are also proposed to reduce the ripple current in dc-link capacitor, these converters are popular because of eliminating circulating current and these converters have soft switching issues [5-8]. There are so many dc-dc converters were used for input PFC stage, conventional boost, bridgeless boost, interleaved boost converters are used to maintain the harmonic free input sinusoidal current. Those boost converters had some issues to maintain that harmonic free input current those are high inrush current and the requirement of boost voltage is more than the peak ac line voltage [9].

In this article, the family of buck-boost converters such as buck-boost, CUK, SEPIC and Zeta converters [10], could operate at high input ac line voltages and they provide a flexibility in second stage of dc-dc conversion with a lower regulated dc-link voltage. These converters also have an additional isolated transformer operates at lower flux density, and switching devices have a higher breakdown voltage rating. This paper proposes that CUK converter fed HBLLC and PSFB converter for an EVBC application. This CUK converter does not have high inrush current issues compared to the boost converter due to the presence of an intermediate capacitor and dc-link voltage was independent. The control algorithm of CUK converter was operated in discontinuous inductor conduction mode to design those parameters [11] [12]. Various control techniques like digital control techniques of CUK converters are also proposed [13].

II. PROPOSED CUK CONVERTER FED HBLLC RESONANT CONVERTER

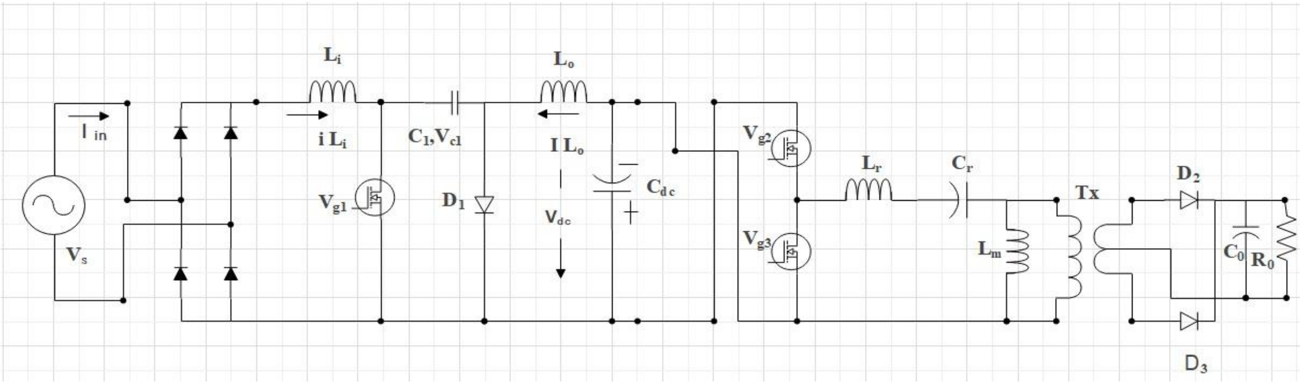

Fig. 2: Configuration of CUK converter fed isolated HBLLC

The above fig.2 shows the proposed converter of CUK converter fed isolated HBLLC converter for an EV charger application. The input stage of power factor correction is done by CUK converter. In that, the input inductor (L_i) was operated in CCM, and output inductor (L_o) was operated in DCM mode, these two form a voltage follower to improve input current shaping to sinusoidal.

The voltage across the intermediate capacitor (V_{c1}) was also in CCM. The voltage across the capacitor C_{dc} was the output voltage V_{dc} and input to the HBLLC converter. The HBLLC resonant converter steps down the dc-link voltage V_{dc} to isolate voltage V_o that is required for an EV charger application. [14]

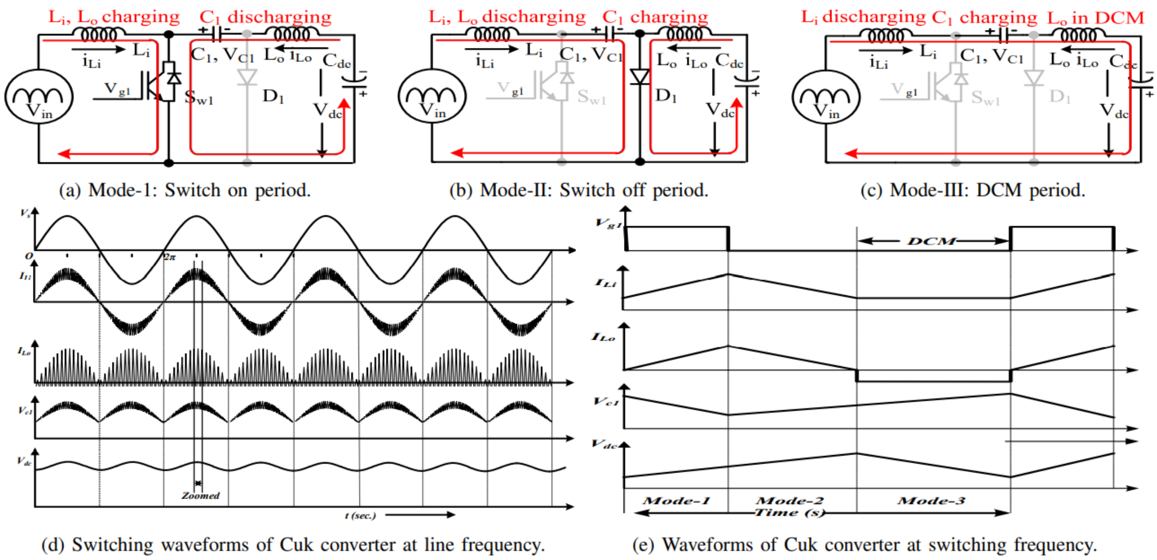

(a) Mode-1: Switch on period. (b) Mode-II: Switch off period. (c) Mode-III: DCM period.

(d) Switching waveforms of Cuk converter at line frequency. (e) Waveforms of Cuk converter at switching frequency.

Fig. 3: Modes of Operation of CUK converter in DCM

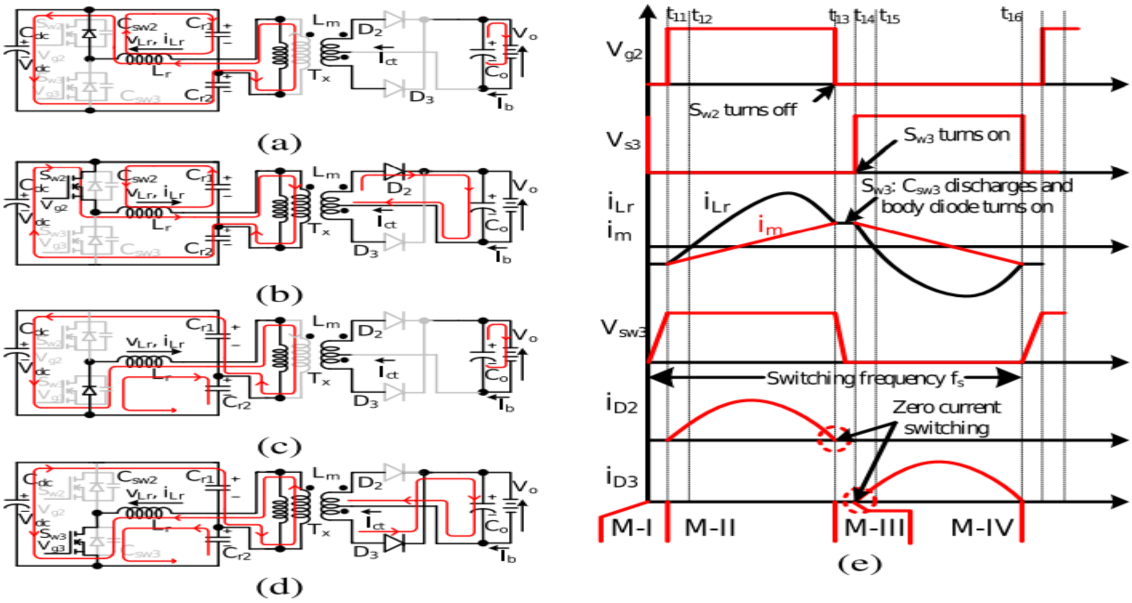

Fig. 4: Operating Modes of HBLLC Converter a) Mode 1 b) Mode 2 c) Mode 3 d) Mode 4 e) Switching Waveforms of the HBLLC converter

III. PROPOSED CUK CONVERTER FED ISOLATED PSFB CONVERTER

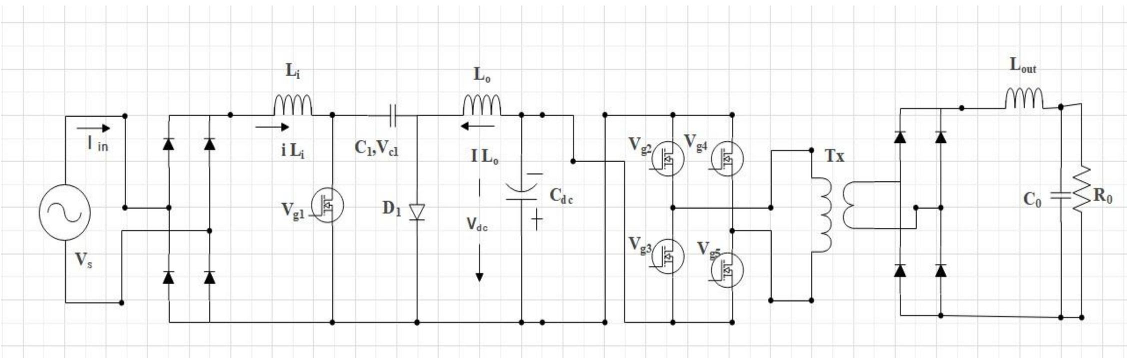

Fig. 5: Configuration of CUK Converter fed isolated PSFB

The above fig. 5 shows the proposed converter of CUK converter fed isolated PSFB. Here the power factor correction was achieved by the CUK converter, here input inductor operated in CCM mode and output inductor operated in DCM mode. The intermediate capacitor voltage also operates in CCM mode. The dc-link voltage V_{dc} was act as input to the isolated PSFB converter. In this the second stage of conversion happens by step down the high voltage V_{dc} to isolated low voltage V_o required for an EV application.

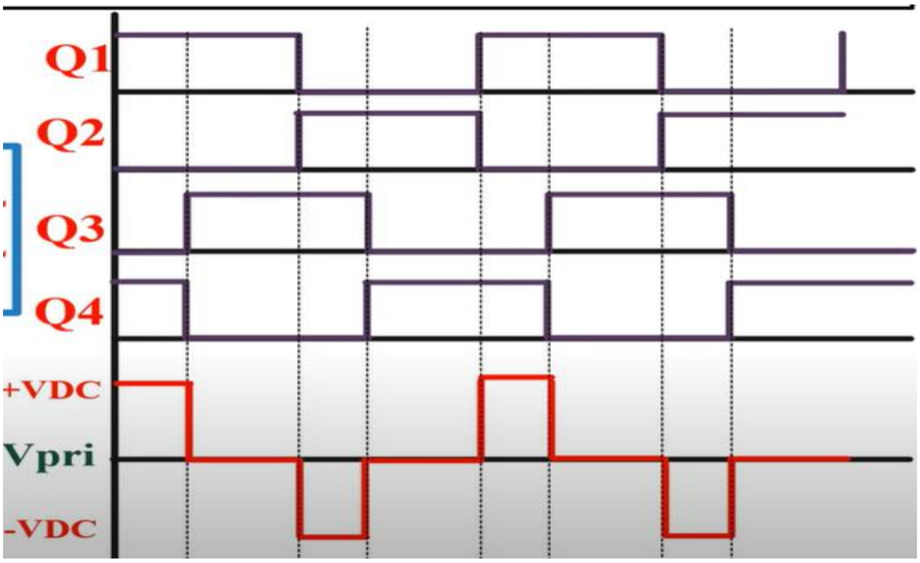

Fig. 6: Switching Waveforms of PSFB converter.

IV. DESIGINING OF PROPOSED CONVERTER

a) Designing of CUK Converter:

During Mode-1 shown in the above figure 4.2, the switch is in ON condition and the diode was in OFF condition. Therefore, the expression of the input inductor L_i, can be given as:

$$L_i = \frac{v_{in} D}{\eta(I_{in} f_S)} = \frac{RD}{\eta f_s} = \frac{1}{\eta f_s}\frac{V_S^2}{P_{in}}\frac{v_0}{v_0 + v_{in}} \quad 1$$

$$L_i = \frac{220^2 * 300}{0.6 * 30000 * 580 * (300 + 311)} = 2.276\text{mH}$$

During Mode-2 shown in the above figure 4.3, the switch is in OFF condition, the current through the output inductor Lo decreases linearly to zero and the diode becomes reverse biased. An inductor Lo current becomes negative during each switching period due to the discontinuous conduction mode (DCM) of operation. To ensure the DCM operation of CUK converter we must choose the critical conduction parameter can be given as:

$$K_{a\_crit} = \frac{0.5}{\left(1 + \frac{V_0}{\sqrt{2}V_{in}}\right)^2} = 0.1296 \quad 2$$

The conduction parameter (K_a) we must choose $K_a < K_{a\_crit}$. K_a must be two-third of K_{a_crit}. So, K_a should be 0.086 and L_{eq} can be given as:

$$L_{eq} = \frac{R_0 K_a}{2f_s} = \frac{(300^2/580)0.086}{2*30000} = 222.4\mu\text{H} \quad 3$$

The Value of output inductor Lo in DCM can be given as:

$$L_o = \frac{L_{eq}L_i}{L_{eq} + L_i} = 0.2464\ \mu H \quad (4)$$

The Value of Intermediate Capacitor C1 in DCM can be given as:

$$C_1 = \frac{1}{\omega_r^2(L_i + L_o)} = 405.54\ nF \quad (5)$$

Where $\omega_r = 2\pi f_r$ was called resonant frequency and $f_L < f_r < f_s$ then we resonant frequency (f_r) was chosen as 5000 Hz. For a maximum voltage ripple (δ) of 3%, then the DC-link capacitor was given by

$$C_{dC} = \frac{I_{dc}}{2\omega_L \delta V_0} = 342\mu F \quad (6)$$

b) Designing of HBLLC converter:

The input voltage of HBLLC converter was loosely regulated to 300 V from the output of CUK Converter. The output voltage of LLC converter is required to charge an EV within a range of 48-60 V. The power rating was 580 W. Thus, the turns ratio of the transformer was given as:

$$n = \frac{0.5 * V_{in}}{V_0} = \frac{0.5 \times 300}{55} = 2.72 \quad (7)$$

The peak current through LLC series resonant converter was given as:

$$i_{L_{r_{peak}}} = \frac{\Pi \times P_0}{V_{dc}} = 6.07 \quad (8)$$

The resonant capacitor was given as:

$$C_r = \frac{i_{L_{r_{Peak}}}}{\Pi * f_s * V_0} = 64 \cdot 4nF \quad (9)$$

For a resonant frequency of 100 kHz, the value of resonant inductor was given as:

$$L_r = \frac{1}{(2\Pi f_r)^2 C_r} = 39.33\mu H \quad (10)$$

Let us assume the magnetization ratio of 6, then the value of magnetizing inductance was given as:

$$L_m = 6 * L_r = 235 \cdot 98\mu H \quad (11)$$

c) Designing of PSFB Converter:

The input voltage to PSFB was output of the CUK converter that was V_{dc} and it was loosely regulated at 300 V. The output voltage was range of 48-55 V. The power rating was 580 W.
Then the transformer turns ratio was given as:

$$\frac{N_s}{N_p} = \frac{52.5}{300} = 0.2 \quad (12)$$

The Output inductor value by considering current ripple of 4% and V_L was 22 V and duty cycle of 0.343, given as:

$$L_{out} = \frac{V_L D T_s}{i_{r_i}} = 40 \cdot 25\mu H \qquad \textbf{13}$$

V. CONTROL OF CONVERTER:

a) Control of CUK Converter**:**

The control diagram of CUK converter was shown below:

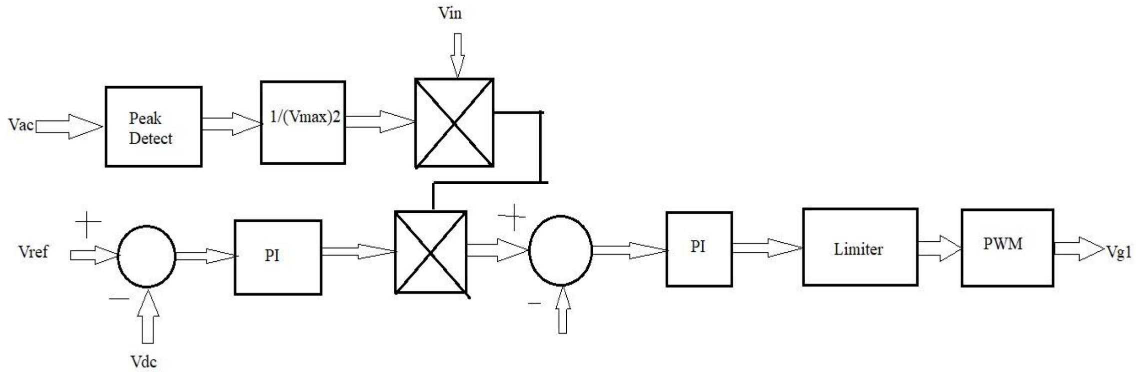

Fig. 7: control of CUK converter

In this it detects the RMS value and multiply with output of PI controller connected to the difference in voltage of reference to dc-link voltage and error in current will connect to PI controller and control the PWM signal of gate.

b) Control of HBLLC converter:

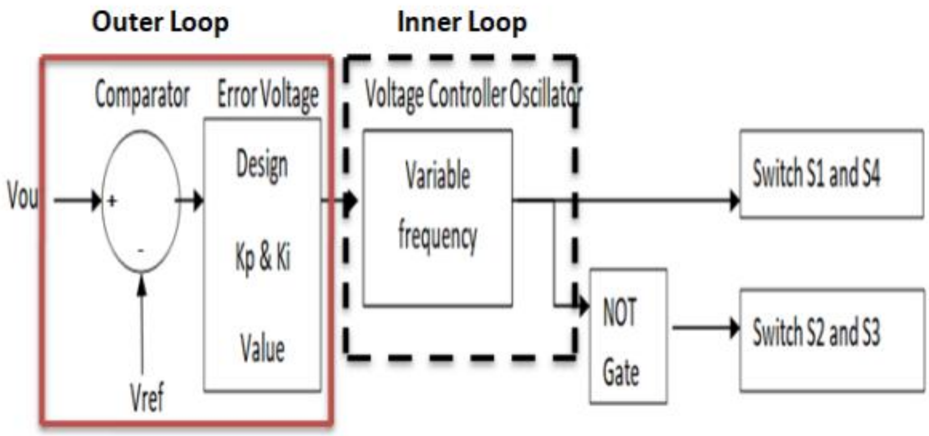

Fig. 8: Control loop diagram of HBLLC Converter

The above block diagram in Fig. 8 shows the control loop of HBLLC resonant converter. The outer loop forms voltage feed back loop and inner loop forms VCO.

The sensed output Voltage Vo, the VCO can generate the drive signals based on the given error voltage and compared it to the reference voltage. [15]

c) Control of PSFB Converter:

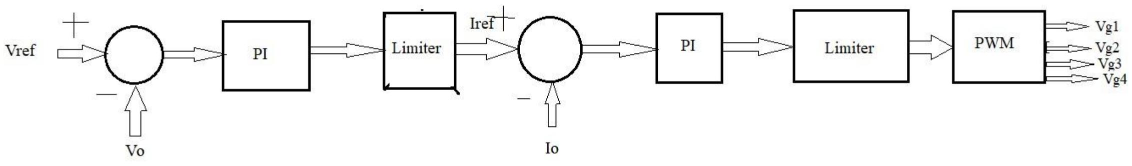

Fig. **9**: Control loop diagram of PSFB Converter

The voltage feedback loop compares the reference voltage with the output voltage Vo, and the current controller loop compares the reference current coming from PI controller block and output current. These error current controls the phase shift of the switches and gives it to PWM block.

VI. RESULTS AND DISCUSSIONS

The above two converters show in fig. 2 and fig. 5 are simulated in MATLAB/ Simulink by using the control techniques discussed above and the results are shown below:

a) Steady State Performance of CUK, HBLLC and PSFB Converters:

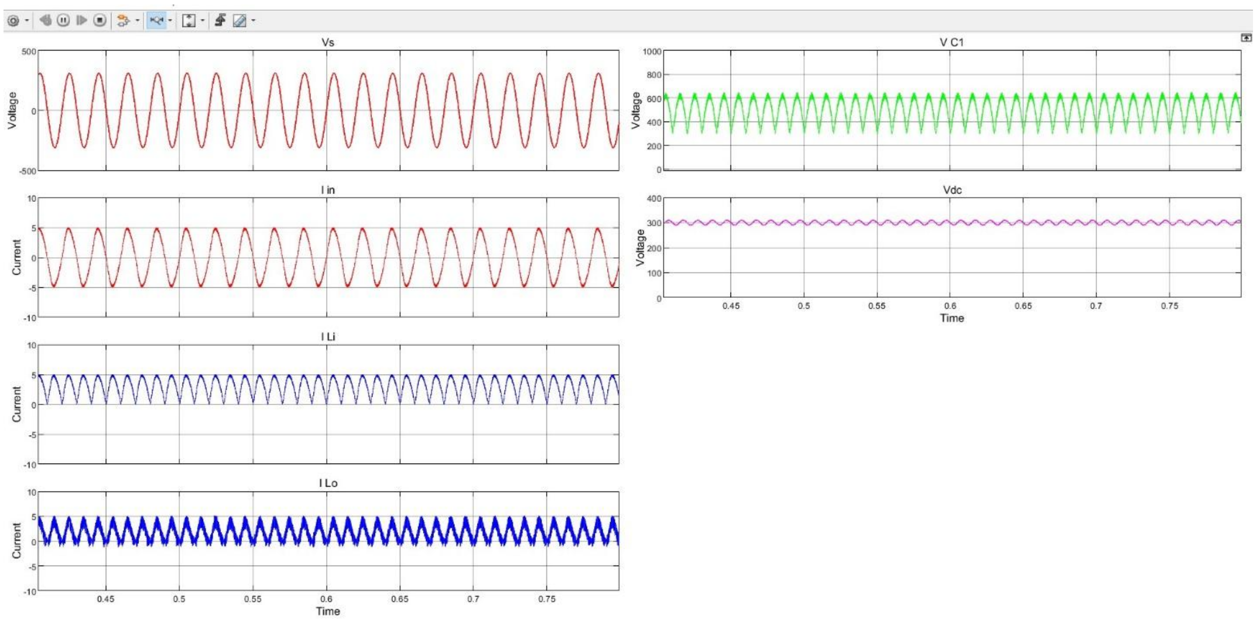

Fig. 10: CUK Converter performance at switching frequency

The above fig. 10 show the CUK converter performance when it is simulated at power rating of 580 w and 220 V_{rms}. The input current exactly matches the sinusoidal shape as like as input voltage and the dc-link voltage were exactly regulated.

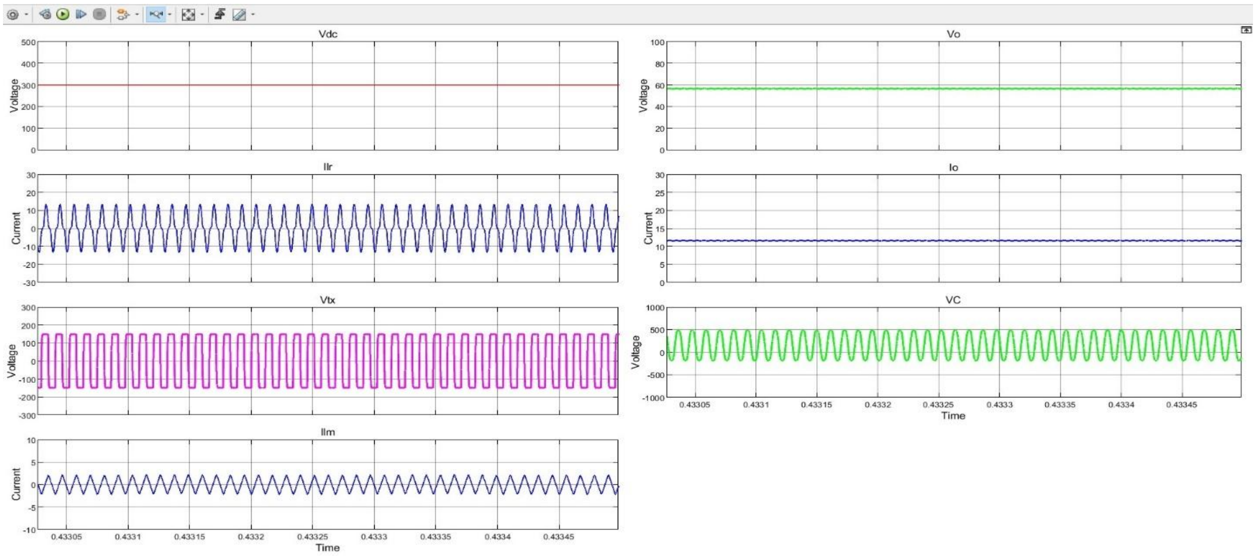

Fig. 11: HBLLC converter performance at switching frequency

The above fig. 11 shows the performance of HBLLC converter when it simulated at rated power of 580 W and 220 V $_{rms}$. The output voltage of transformer (Vtx) was perfectly square and output voltage and output current was almost maintained constant.

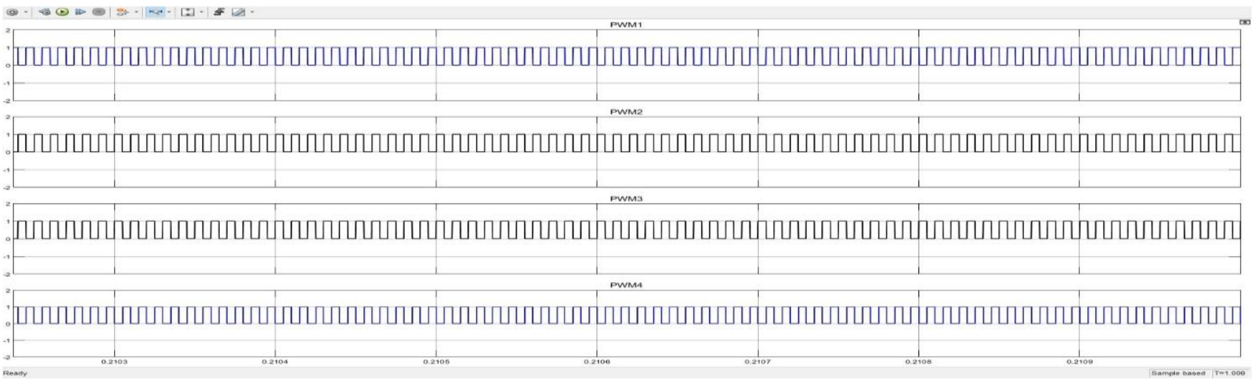

Fig. 12: GATE Signals of Switches of PSFB Converter

The above fig. 12 shows the gate signals of PSFB converter, by observing that figure there is a phase shift of 180 degrees between PWM1, PWM4 and PWM2, PWM3.

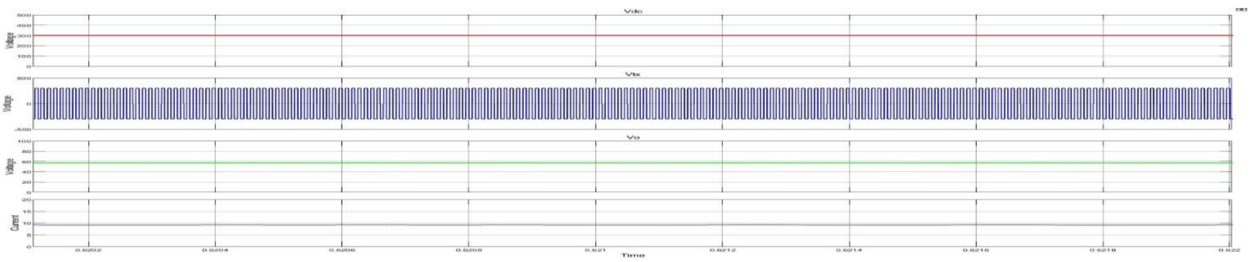

Fig. 13: Performance of PSFB Converter

b) Dynamic Performance of CUK Converter with HBLLC converter:

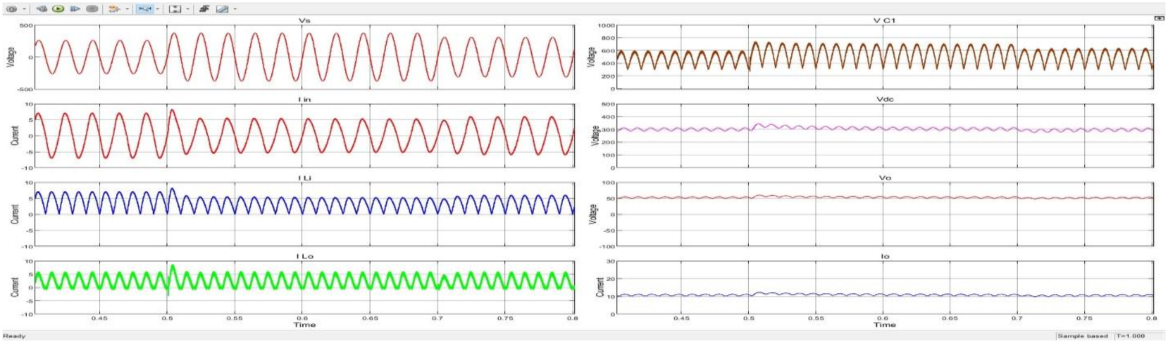

Fig. 14: Performance of CUK+HBLLC at R Load

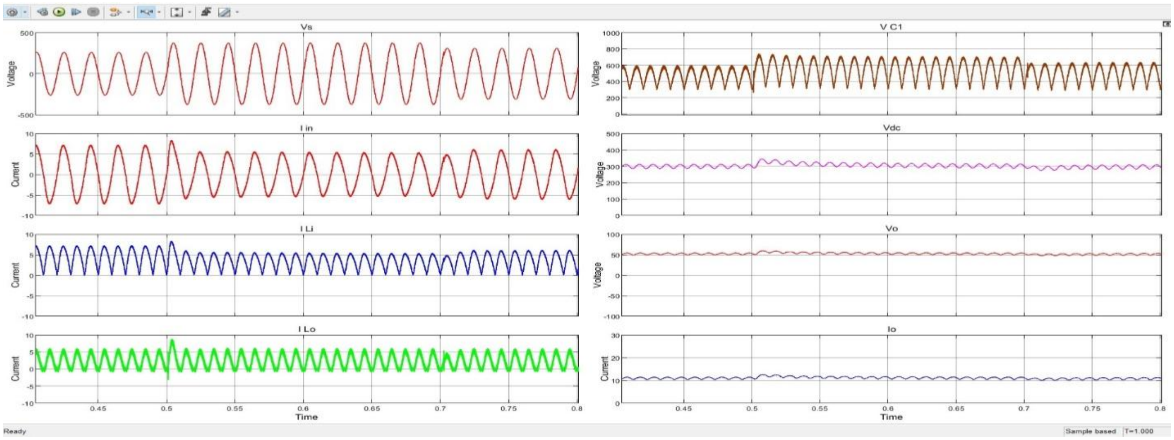

Fig. 15: Performance of CUK+HBLLC at RL Load

The dynamic performance was performed at 185 V $_{rms}$ from 0 to 0.5s and 265 V $_{rms}$ from 0.5 to 0.7s and finally from 220 V $_{rms}$ from 0.7 to 1s and the results are shown in above fig. 14 and fig. 15.
The THD and Power Factor Values are tabulated as below:

Table -1: THD and PF of CUK+HBLLC at R Load

Voltage Level	THD	Input Power Factor
185 Vrms	4.89%	0.9987
220 Vrms	5.65%	0.9981
265 Vrms	6.53%	0.9973

Table-2: THD and PF of CUK+HBLLC at RL Load

Voltage Level	THD	Input Power Factor
185 Vrms	5.01%	0.9987
220 Vrms	5.85%	0.9981
265 Vrms	6.78%	0.9973

c) Dynamic performance of CUK converter with PSFB Converter:

d)

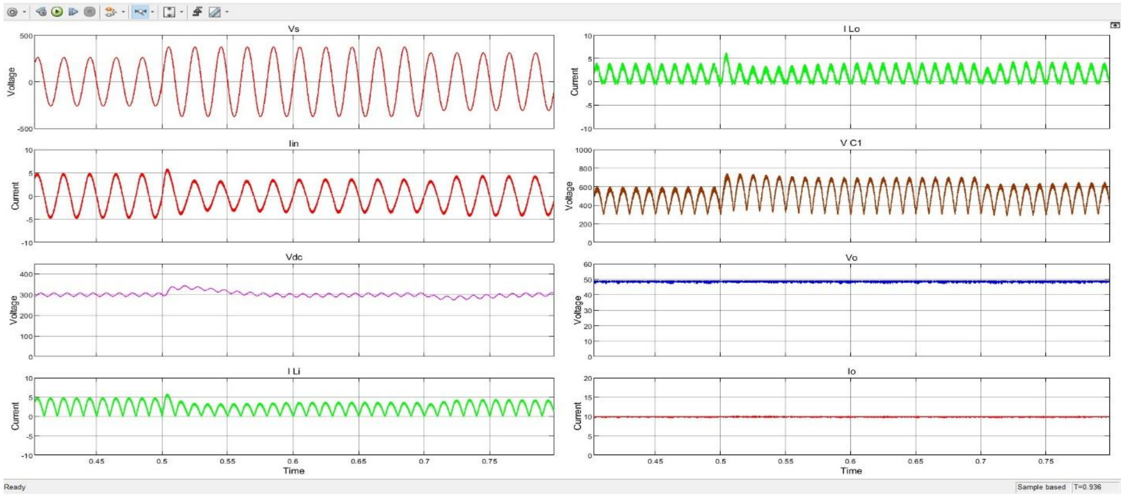

Fig. 16: Performance of CUK + PSFB at R Load

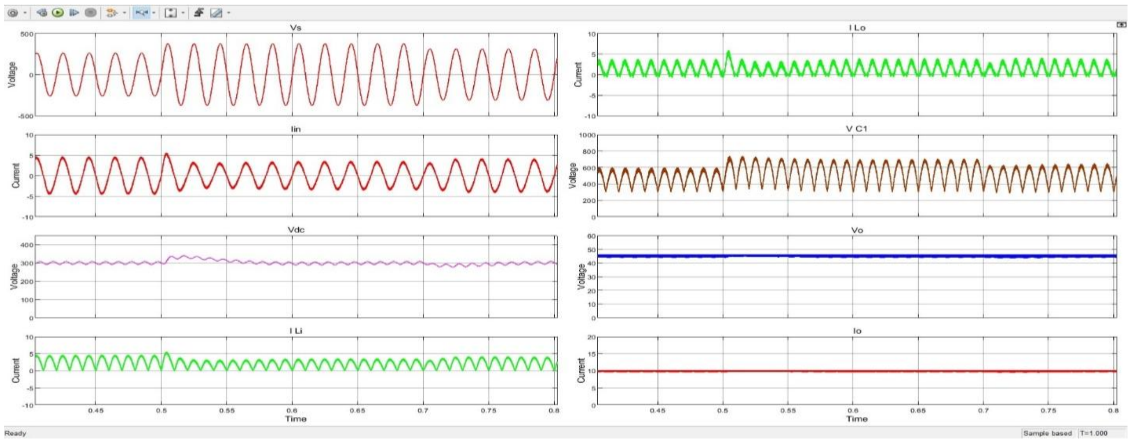

Fig. 17: Performance of CUK+PSFB at RL Load

The dynamic performance was performed at 185 V $_{rms}$ from 0 to 0.5s and 265 V $_{rms}$ from 0.5 to 0.7s and finally from 220 V $_{rms}$ from 0.7 to 1s and the results are shown in above fig. 16 and fig. 17.The THD and Power Factor Values are tabulated as below:

Table-3: THD and PF values of CUK+PSFB at R Load:

Voltage Level	**THD**	**Input Power Factor**
185 Vrms	3.68%	0.9987
220 Vrms	4.25%	0.9981
265 Vrms	4.74%	0.9973

Table-4: THD and PF values of CUK+PSFB at RL Load:

Voltage Level	THD	Input Power Factor
185 Vrms	4.01%	0.9987
220 Vrms	4.35%	0.9981
265 Vrms	5.15%	0.9973

VII. CONCLUSION

In this article, the performance of CUK converter with HBLLC converter and CUK converter with PSFB converter was designed, developed and analyze the performance of the individual converters was simulated using MATLAB/SIMULINK and results are discussed above. Here, the frequency control loop was developed to control the HBLLC operating at different frequencies. The combination of those at different loads. We analyze the performance of converters by setting up the transients and we found smooth waveforms and without oscillations.

VIII. REFERENCES

[1] A. Khaligh and M. D'Antonio, "Global trends in high-power on-board chargers for electric vehicles," IEEE Trans. Veh. Technol., vol. 68, no. 4, pp. 3306–3324, Apr. 2019.

[2] S. S. Williamson, A. K. Rathore, and F. Musavi, "Industrial electronics for electric transportation: Current state-of-the-art and future challenges," IEEE Trans. Ind. Electron., vol. 62, no. 5, pp. 3021–3032, May 2015.

[3] K. Fahem, D. E. Chariag, and L. Sbita, "On-board bidirectional battery chargers' topologies for plug-in hybrid electric vehicles," in Proc. Int. Conf. Green Energy Convers. Syst., 2017, pp. 1–6.

[4] N. Hassanzadeh, F. Yazdani, S. Haghbin, and T. Thiringer, "Design of a 50-kW phase-shifted full-bridge converter used for fast charging applications," in Proc. IEEE Veh. Power Propulsion Conf., 2017, pp. 1–5.

[5] Y.-K. Lo, C.-Y. Lin, M.-T. Hsieh, and C.-Y. Lin, "Phase-shifted full-bridge series-resonant DC-DC converters for wide load variations," IEEE Trans. Ind. Electron., vol. 58, no. 6, pp. 2572–2575, Jun. 2011.

[6] I.-O. Lee and G.-W. Moon, "Phase-shifted PWM converter with a wide ZVS range and reduced circulating current," IEEE Trans. Power Electron., vol. 28, no. 2, pp. 908–919, Feb. 2013.

[7] J. M. Miller, O. C. Onar, and M. Chinthavali, "Primary-side power flow control of wireless power transfer for electric vehicle charging," IEEE J. Emerg. Sel. Topics Power Electron., vol. 3, no. 1, pp. 147–162, Mar. 2015

[8] S. Samanta, A. K. Rathore, and D. J. Thrimawithana, "Analysis and design of current-fed half-bridge (C)(LC)–(LC) resonant topology for inductive wireless power transfer application," IEEE Trans. Ind. Appl., vol. 53, no. 4, pp. 3917–3926, Jul./Aug. 2017.

[9] M. Alam, W. Eberle, D. S. Gautam, C. Botting, N. Dohmeier, and F. Musavi, "A hybrid resonant pulse-width modulation bridgeless AC–DC power factor correction converter," IEEE Trans. Ind. Appl., vol. 53, no. 2, pp. 1406–1415, Mar./Apr. 2017.

[10] B. Singh, B. N. Singh, A. Chandra, K. Al-Haddad, A. Pandey, and D. P. Kothari, "A

review of single-phase improved power quality AC-DC converters," IEEE Trans. Ind. Electron., vol. 50, no. 5, pp. 962–981, Oct. 2003.

[11] A. Anand and B. Singh, "Design and implementation of PFC Cuk converter fed SRM drive," IET Power Electron., vol. 10, no. 12, pp. 1539–1549, 2017.

[12] A. J. Sabzali, E. H. Ismail, M. A. Al-Saffar, and A. A. Fardoun, "New bridgeless DCM SEPIC and Cuk PFC rectifiers with low conduction and switching losses," IEEE Trans. Ind. Appl., vol. 47, no. 2, pp. 873–881, Mar./Apr. 2011.

[13] S. Dian, X. Wen, X. Deng, and S. Zhang, "Digital control of isolated Cuk power factor correction converter under wide range of load variation," IET Power Electron., vol. 8, no. 1, pp. 142–150, 2014.

[14] Rahul Pandey, Bhim Singh, "Resonant LLC converter for E-Bike Charger", International conference on Electrical, Electronics and Computer Engineering, 8-10 Nov 2019.

[15] Amit Singh Tandon, Naveen Yalla, AVJS Praneeth, Piyush Kumar, Vijay Anand, "Design of GaN based 72V,3.3KW LLC Resonant Converter for on-board EV Charger", IEEE Madras section Conference, 27-28 Aug 2021.